Entrained flow gasification: experiments and mathematical modelling based on RANS

M. Dammann[*,1,2,3], M. Mancini[3], S. Fleck[2], R. Weber[3] and T. Kolb[1,2]

* maximilian.dammann@kit.edu, maximilian.dammann@tu-clausthal.de

[1] *Karlsruhe Institute of Technology (KIT), Engler-Bunte-Institute, Fuel Technology (EBI ceb), Engler-Bunte-Ring 1, 76131 Karlsruhe, Germany*

[2] *Karlsruhe Institute of Technology (KIT), Institute for Technical Chemistry, Gasification Technology (ITC vgt), Herrmann-von-Helmholtz-Platz 1, 76344 Eggenstein-Leopoldshafen, Germany*

[3] *Clausthal University of Technology, Institute for Energy Process Engineering and Fuel Technology (IEVB), Agricolastrasse 4, 38678 Clausthal-Zellerfeld, Germany*

Abstract

Entrained flow gasification of biomass has become one of the promising technologies for the production of fuels and chemicals in a closed carbon cycle economy. Due to the complexity of the conversion of low-rank fuels to high-quality synthesis gas and due to the lack of experimental data inside entrained flow gasifiers, there is still a need for a better understanding of the physical and thermo-chemical processes during entrained flow-gasification. In order to close this gap, the bioliq® process [1]) has been constructed at Karlsruhe Institute of Technology (KIT). In parallel, the research network Helmholtz Virtual Institute for Gasification Technology (HVIGasTech) [2] has been established. Its primary focus is the development of a numerical model for the description of the entrained flow gasification of biomass at both atmospheric-pressure and high-pressure conditions.

This paper focuses on the recent experimental and numerical results of four campaigns carried out at the atmospheric research entrained flow gasifier REGA [3]. The two first campaigns (REGA-glycol-T1, REGA-glycol-T2) used ethylene glycol as model fuel; the two others (REGA-slurry1-T2, REGA-slurry2-T2) applied model slurries (90 % ethylene glycol + 10 % wood-char and 70 % ethylene glycol + 30 % wood-char). In each of these campaigns, radial profiles of gas phase composition (CH_4, CO, CO_2, H_2) and gas phase temperature were measured at burner distances of 300 mm and 680 mm. The experimental data sets have been used for the validation of the RANS based numerical model. The model assumes a steady state and includes turbulence-chemistry interaction described by the Eddy Dissipation Concept (EDC) in combination with one of two global reaction mechanisms for the entrained flow gasification of ethylene glycol: the HVI1 mechanism and the extended Jones-Lindstedt mechanism [4]. Reaction rates for the devolatilisation and the heterogeneous reactions of wood-char with CO_2 and H_2O are derived from measurements [5,6].

The numerical results concerning the entrained flow gasification of ethylene glycol show that both global mechanisms predict the gas phase compositions well and overpredict the gas phase temperatures slightly. The model based on the HVI1 mechanism has advantages in the near-burner region and in computing time. The numerical results for the entrained flow gasification of slurry deviate from the experimental results concerning the gas phase composition. Experimental results suggest a higher carbon conversion of wood-char than predicted. Sensitivity studies also emphasize that higher reaction rates concerning the heterogeneous reactions are required for the numerical model. In addition to that, numerical errors in balance of elements are a significant source of error. Therefore, further research has already been initiated to reinvestigate and to improve both the numerical accuracy and the heterogeneous kinetics.

Introduction

Entrained flow gasification considers the conversion of carbonaceous fuels to synthesis gas using a gasification medium. While coal, petroleum and petroleum coke have been the significant fuels for entrained flow gasification in the last century, nowadays liquid and suspension fuels based on biomass or waste are getting an important role due to the global objective to close the carbon cycle [7]. However, the research level on entrained flow gasification of biomass and waste lags behind that of coal, petroleum and petroleum coke. Therefore, several research projects have been carried out in the

last decades (e.g. HVIGasTech [2]) and several pilot plants for the entrained flow gasification of biomass based fuels have been constructed (e.g. bioliq[©] [1]) to investigate the physical and thermo-chemical processes inside of entrained flow gasifiers. These steps include atomisation, evaporation, decomposition, devolatilisation, homogenous and heterogeneous gasification, ash transformation and slagging (see Fig. 1). Because not all of these processes can be investigated inside pilot plants even if they are equipped with extensive measurement techniques and have got optical access to the reactor chamber, lab scale plants are further key tools in research of entrained flow gasification.
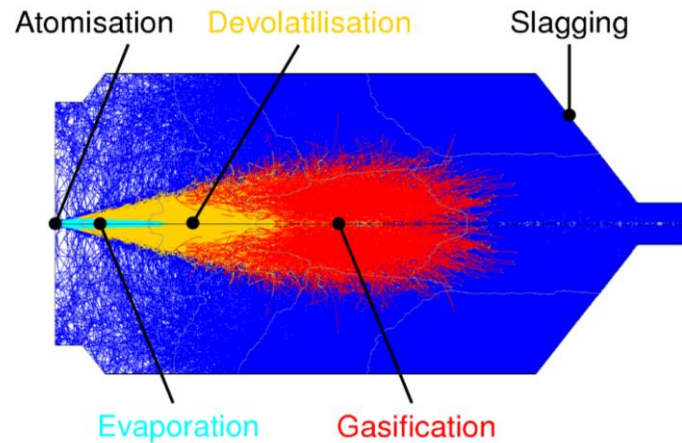

Figure 1. Particle trajectories and process steps of gasification shown for the entrained flow gasifier bioliq EFG.

At Karlsruhe Institute of Technology, several lab scale plants and one pilot plant have been established with the objective to improve sub-models and to develop an overall mathematical model for entrained flow gasification of biomass at both atmospheric and high pressure conditions. While gasification experiments at high-pressure conditions are carried out at the bioliq EFG, the research entrained flow gasifier REGA is used for gasification experiments at atmospheric conditions including measuring radial profiles of gas phase composition and gas phase temperature inside. Furthermore, the atmospheric spray test rig ATMO [3] and the drop tube reactor DTR [6] are employed for atomisation and kinetic experiments at atmospheric conditions, respectively.

Due to the long history of entrained flow gasification, a large amount of experimental and/or modelling and simulation studies were already carried out (see e.g. [8-12]). Most of the experiments focus on gas phase composition and gas phase temperature at outlet. Experimental data sets from inside of entrained flow gasifiers are limited. At Brigham Young University (BYU) [9], an atmospheric entrained flow gasifier was operated with coal and radial profiles of gas phase composition and gas phase temperature were measured

The numerous modelling studies can be differentiated in those (see e.g. [8]) employing one-dimensional models and in those (see e.g. [9-12]) applying CFD software (e.g. in-house, Fluent, OpenFOAM). The latter are quite similar in sub-models and differentiate mainly in geometry, operating conditions and fuel properties. Transport equations are based on RANS and the turbulence models are described by one of the common models (e.g. standard k-ε, SST k-ω, RSM). Radiation was often described using discrete-ordinates method, P1 model or discrete transfer radiation model. Global reaction mechanisms (Westbrook and Dryer [13], Jones and Lindstedt [14]) are usually employed for the homogeneous kinetics and the reactions of the typically solid fuel with CO_2, H_2, H_2O and O_2 are assumed for the heterogeneous kinetics. The reaction rates for the latter kinetics and the reaction rate of the devolatilisation process were derived from either literature data or measurements (see e.g. Brown et al. [9]).

This paper is part of a series of publications either published recently in journals [3,4,15] or presented at meetings of sections of the Combustion Institute [16-19]. It gives an overview of the older and the newest results concerning the entrained flow gasification of model fuels at atmospheric conditions and of the challenges to obtain reliable results.

Experiments

The REGA (see Fig. 2 and for details see Fleck et al. [3]) is a reactor consisting of a ceramic tube with an inner diameter of 280 mm and a length of 3000 mm. Multiple ports are arranged along the reactor axis. The side walls of the reactor can be heated electrically up to a temperature of 1200 °C. The top of the reactor contains a twin-fluid external mixing nozzle at the centre and is movable along the reactor axis which allows measurements in a certain range of burner distances. The REGA can be operated with liquid and suspension fuels having a thermal input of 60 kW. Air used as gasification medium can be enriched with oxygen up to volume fractions of 70 %. The mass flow rate of the fuel stream is determined using a Coriolis mass flow controller and the volume flow rates of the gas streams are measured with thermal flow controllers based on hot wire anemometry. Due to reactor pressures of 1 to 2 mbar below the ambient pressure, ambient air infiltrates the reactor. The mass flow rate of this stream cannot be measured and is estimated based on the balance of elements.

Gas samples are extracted from the reactor using cooled steel probes with a ceramic tip and are filtered. The gas phase composition of a part of the sample is analysed for the dry volume fractions of CH_4, CO, CO_2 and H_2 using standard gas analysers or a µGC. Gas phase temperatures at fixed positions along the reactor axis are determined using ceramic shielded type S thermocouples; gas phase temperatures at radial profiles are measured with type B double bead thermocouples, which allow temperature correction by taking into account the impact of radiation.
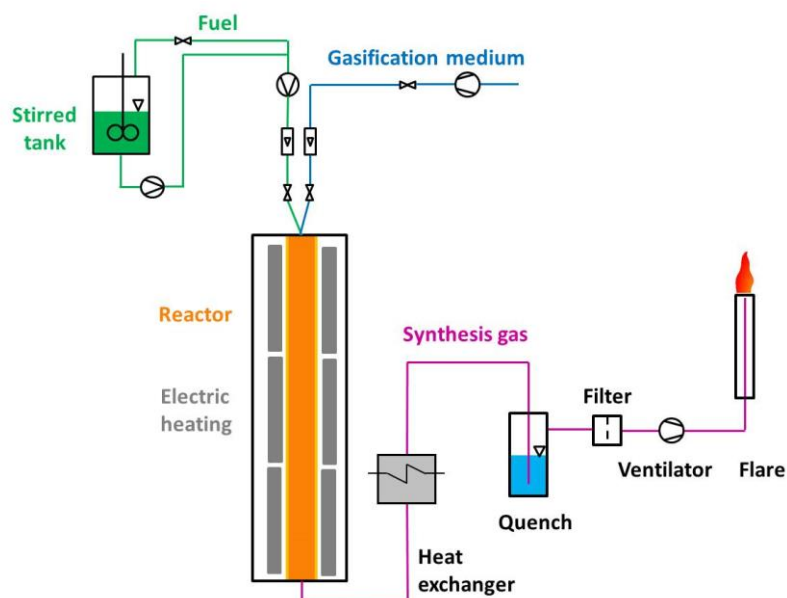

Figure 2. Process scheme of the entrained flow gasifier REGA [3].

Four experimental campaigns were carried out. In two campaigns, ethylene glycol was applied as model fuel. The objective was to investigate the homogenous gasification using settings based on low and high adiabatic temperatures and to develop and validate a simplified reaction mechanism. In the other two campaigns, mixtures of ethylene glycol and wood char (90 % ethylene glycol + 10 % wood-char and 70 % ethylene glycol + 30 % wood-char) were employed. The settings of both campaigns are characterised by adiabatic temperatures similar to the adiabatic temperature of the second campaign. Table 1 gives an overview of the mass flow rates measured in each campaign or calculated for each campaign (see also Dammann et al. [19]). The given mass flow rate of nitrogen in the first campaign is due to purging of sight glasses at one port.

In each campaign, radial profiles of gas phase composition and gas phase temperature at burner distances of 300 mm and 680 mm were measured.

Table 1. Mass flow rates and adiabatic temperatures [4,19].

Campaign	Mass flow rate in kg/h					Adiabatic Temperature in K
	Fuel	O_2	Air	N_2	Inf. Air	
REGA-glycol-T1	12.56	7.11	9.04	0.64	1.93	2273
REGA-glycol-T2	12.42	6.54	3.76	0	0.59	1973
REGA-slurry1-T2	12.45	6.99	3.66	0	0.46	2041
REGA-slurry2-T2	12.76	7.77	2.65	0	0.64	1971

Mathematical modelling

The mathematical model developed is based on models that have already been described by Mancini at al. [4]. It uses a two-dimensional, axis-symmetric geometry of the upper part of the REGA and it assumes a steady-state. The model is based on both the RANS and the Euler-Lagrange approach. The RANS and the Euler approach are used for the transport equations of the gas phase, the Lagrange approach is assumed for the balance equations of the dispersed phase.

The transport equations of the gas phase are: the continuity equation, the momentum equation, the energy equation and seven species equations for CH_4, $C_2H_6O_2$, CO, CO_2, H_2, H_2O and O_2. Turbulence is described by the standard k-ε model. Radiation is modelled using the Radiative Transfer Equation solved for $4 \times 8 \times 8 = 256$ directions and assuming a constant absorption coefficient for the gas phase of 0.53m^{-1}. The absorption coefficient has been estimated using the concept of the mean beam length and using HITEMP2010 based line-by-line calculations [4]. Density is described by the ideal gas equation of state and specific enthalpy is based on NASA data. Dynamic viscosity and thermal conductivity are calculated using kinetic theory (Chapman-Enskog, Eucken, Wilke).

The boundary conditions at inlet are based on the flow rates and temperatures measured in the experimental campaigns. The no-slip condition, the linear law of the wall due to wall distances $y^+ < 5$ and a refractory temperature of 1200°C in combination with a one-dimensional thermal resistance for the refractory are applied at wall. Furthermore, source terms are implemented for the upper fluid region near the wall in order to describe the infiltration air.

The reactions of the gas phase are calculated based on the Eddy Dissipation Concept (EDC) and one of two global reaction mechanisms developed for the entrained flow gasification of ethylene glycol: the extended Jones-Lindstedt (eJL) mechanism or the HVI1 mechanism [4]. The heterogeneous reactions considered are the reactions describing devolatilisation, the Boudouard reaction and the water-gas reaction. Their reaction rates are based on measurements at Karlsruhe Institute of Technology [5] and RWTH Aachen [6] and the equations

$$dX_{\text{dev}}/dt = k_0 \exp(-E_a/(R\,T_{\text{part}}))\,(1 - X_{\text{dev}}) \tag{1}$$

and

$$dX_{\text{gas}}/dt = \Sigma_r\,\eta_r\,k_r\,(1 - X_{\text{gas}})^n \quad \text{for } r = CO_2, H_2O \tag{2}$$

where X_{dev} and X_{gas} are the degrees of conversion due to devolatilisation and gasification, respectively, t is the time, k_0 is the pre-exponential factor, E_a is the molar activation energy, T_{part} is the particle temperature, η is the effectiveness factor, k is the rate of coefficient described by the Langmuir-Hinshelwood approach and n is a dimensionless constant.

The dispersed phase is modelled by spherical droplets and can consist either of a pure liquid or of a suspension. The pure liquid is assumed in case of the atomisation of ethylene glycol; the suspension is described by solid particles surrounded by a liquid layer in case of the atomisation of mixtures of ethylene glycol and wood-char. The injection of the droplets takes place near the atomiser, i.e. the atomisation is not considered as, for example, in Volume-of-Fluid based models. The injection properties are defined using position, velocity and diameter distributions and are based on atomisation

experiments at ATMO (see Fleck et al [3]). However, other distributions and settings concerning the injection have been tested, too. Turbulent dispersion of the particles has also been considered and is described by the random walk model.

Results

In Fig. 3 and in Fig. 4, experimental and numerical results at two burner distances are depicted for the campaign REGA-glycol-T1 and the campaign REGA-glycol-T2, respectively. The comparison shows that both reaction mechanisms (HVI1 and eJL) are able to predict the experimental results of the campaign REGA-glycol-T2 accurately. Both reaction mechanisms also predict the experimental results of the campaign REGA-glycol-T1 at 680 mm with only small deviations. Temperatures are slightly over predicted by the eJL mechanism. Larger deviations are observed at 300 mm. Only the HVI1 mechanism performs well concerning the gas phase composition.
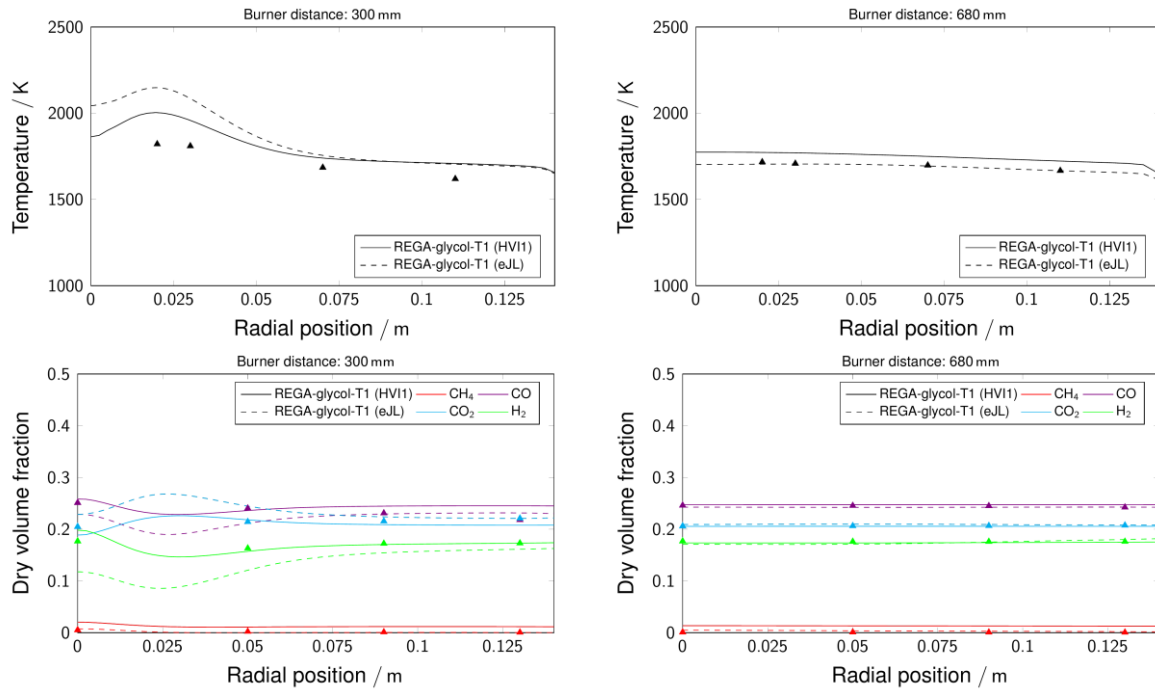

Figure 3. Comparison of the experimental and numerical results of the campaign REGA-glycol-T1 (as reported in Mancini et al. [4]): validation of the numerical results by the experimental results and influence of the global reaction mechanism (HVI1 or eJL) on the numerical radial temperature and dry volume fraction profiles at 300 mm and 680 mm.

In Fig. 5, numerical results based on two different kinds of inlet and injection arrangements are compared for the campaign REGA-glycol-T2. In the default arrangement, the gas phase enters the gasifier through the external mixing nozzle having a high velocity and the particles are injected near the potential core of the gas stream. The disadvantage of this arrangement concerns the spray distribution which is very dense near the reactor axis. Without violating the momentum balance, it is possible to improve this arrangement (at least slightly because the jet/spray angle can still not be predicted). In the new arrangement, the gas stream enters the gasifier through a free-jet nozzle and the particles are injected in the potential core of the gas stream. Such an arrangement improves the numerical results.
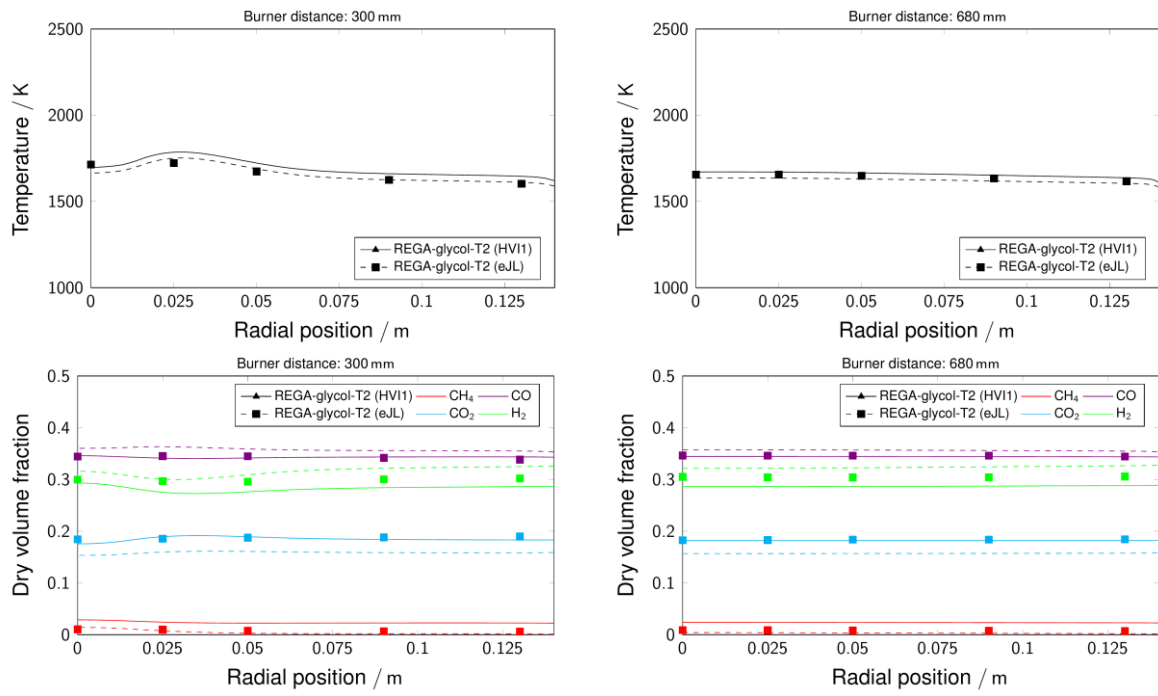
5

Figure 4. Comparison of the experimental and numerical results of the campaign REGA-glycol-T2 (as partially reported in Dammann et al. [19]): validation of the numerical results by the experimental results and influence of the global reaction mechanism (HVI1 or eJL) on the numerical radial temperature and dry volume fraction profiles at 300 mm and 680 mm.
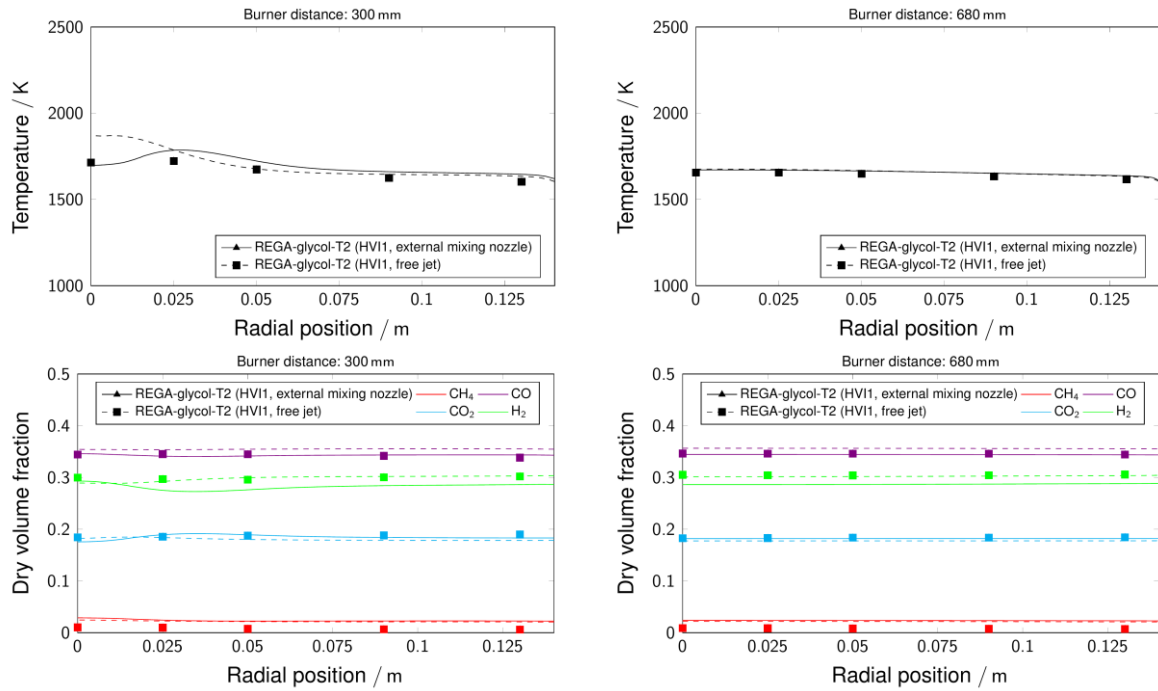

Figure 5. Comparison of the experimental and numerical results of the campaign REGA-glycol-T2 (as partially reported in Dammann et al. [19]): influence of the atomiser modelling (external mixing nozzle vs. free jet) on the numerical radial temperature and dry volume fraction profiles at 300 mm and 680 mm.
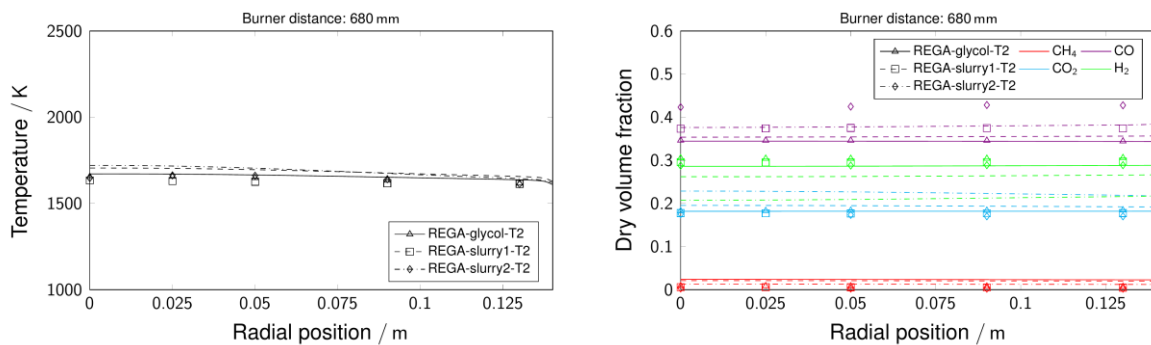
6

Figure 6. Comparison of the experimental and numerical results of the campaign REGA-glycol-T2, REGA-slurry1-T2 and REGA-slurry2-T2 (as partially reported in Dammann et al. [19]).

The influence of wood-char content is shown in Fig. 6. While the gas phase temperature profiles do not differentiate significantly due to the design of the campaigns, the volume fraction profiles changes with clear trends. With increasing wood-char content, the volume fraction profiles of CO increase significantly and the volume fraction profiles of H_2 and CO_2 decrease slightly. These trends can currently not be predicted by the simulations. The volume fraction profiles of CO increase only slightly, the volume fraction profiles of H_2 decrease and those of CO_2 decrease significantly. At the present stage, this is primarily attributed to numerical errors in species balance. Although an appropriate fine mesh is used and significant important quantities do not change with further iterations, i.e. the simulation seems to be converged, errors might be induced due to coupling between gas phase and dispersed phase. Another source of error not related to numerical errors might be the heterogeneous reaction rates. Higher reaction rates for the devolatilisation, the Boudouard reaction and the water gas shift reaction shift the numerical volume fraction profiles to the experimental profiles (not shown).

Conclusions and next steps

Four experimental campaigns on entrained flow gasification of a liquid model fuel (ethylene glycol) and of suspension model fuels (mixtures of ethylene glycol and wood-char) at atmospheric conditions have been carried out and accurate results have been obtained. The results give an insight into the gasification process in the far-flame region and clear trends concerning the gas phase composition and the gas phase temperature with increasing wood-char content.

The modelling and simulation results show that the current RANS based mathematical model is able to predict the gas phase composition and the gas phase temperature in the far-flame region concerning the entrained flow gasification of ethylene glycol and that it cannot predict the trends observed with increasing wood-char content. In order to obtain better numerical results, further research has already been started to decrease the numerical errors and to reinvestigate the heterogeneous reaction rates using new validation experiments in the DTR at Karlsruhe Institute of Technology. Furthermore, the influence of inlet arrangement and injection properties (position, velocity and diameter distribution) on jet/spray angle and the flame has been investigated. The arrangements at the inlet exerts substantially on flow and flame shape (not shown) as well as on the gas phase composition in the near-flame region. Obviously, the influences of the inlet conditions ceases at the burner distance of 300 mm.

References

[1]   Dahmen, N., Abeln, J., Eberhard, M., Kolb, T., Leibold, H., Sauer, J., Stapf, D., Zimmerlin, B.: *The bioliq process for producing synthetic transportation fuels*, WIREs Energy Environment, 6, 2016.

[2]   Kolb, T., Aigner, M., Kneer, R., Müller, M., Weber, R., Djordjevic, N.: *Tackling the challenges*

in modelling entrained-flow gasification of low-grade feedstock, J. Energy Inst., 89, 485-503, 2016.

[3] Fleck, S., Santo, U., Hotz, C., Jakobs, T., Eckel, G., Mancini, M., Weber, R., Kolb, T.: *Entrained flow gasification. Part 1: Gasification of glycol in an atmospheric-pressure experimental rig*, Fuel, 217, 306-319, 2018.

[4] Mancini, M., Alberti, M., Dammann, M., Santo, U., Weber, R., Kolb, T., Eckel, G.: *Entrained flow gasification. Part 2: Mathematical modeling of the gasifier using RANS method*, Fuel, 225, 596-611, 2018.

[5] Kreitzberg, T., Haustein, H.D., Gövert, B., Kneer, R.: *Investigation of gasification reaction of pulverized char under N_2/CO_2 atmosphere in a small-scale fluidized bed reactor*, J. Energy Res. Technol., 138, 42207, 2016.

[6] Stoesser, P., Schneider, C., Kreitzberg, T., Kneer, R., Kolb, T.: *On the influence of different experimental systems on measured heterogeneous gasification kinetics*, Appl. Energy, 211, 582-589, 2018.

[7] Higman C.: *GSTC Syngas Database*, Gasification & Syngas Technologies Conference, Colorado Springs, Colorado, USA, 2018.

[8] Wen, C.Y., Chaung, T.Z.: *Entrainment coal gasification modeling*, Ind. Eng. Chem. Proc. Des. Dev, 18, 684-695, 1979.

[9] Brown, B., Smoot, L.D., Smith, P.J., Hedman, P.O.: *Measurement and prediction of entrained-flow gasification processe*s, AlChE J., 34, 435-446, 1988.

[10] Chen, C., Horio, M., Kojima, T.: *Numerical simulation of entrained flow coal gasifiers. Part I: modeling of coal gasification in an entrained flow gasifier*, Chem. Eng. Sci., 55, 3861-3874, 2000.

[11] Watanabe, H., Otaka, M.: *Numerical simulation of coal gasification in entrained flow coal gasifier*, Fuel, 85, 1935-1943, 2006.

[12] Marklund, M., Tegman, R., Gebart, R.: *CFD modelling of black liquor gasification: Identification of important model parameters*, Fuel, 86, 1918-1926, 2007.

[13] Westbrook, C.K., Dryer, F.L.: *Simplified reaction mechanisms for the oxidation of hydrocarbon fuels in flames*, Combust. Sci. Technol., 27, 31-43, 1981.

[14] Jones, W.P., Lindstedt, R.P.: *Global reaction schemes for hydrocarbon combustion*, Combust. Flame, 73, 233-249, 1988.

[15] Eckel, G., Le Clercq, P.C., Kathrotia, T., Sänger, A., Fleck, S., Mancini, M., Kolb, T., Aigner, M.: *Entrained flow gasification. Part 3: Insight into the reactor near-field by Large Eddy Simulation with detailed chemistry*, Fuel, 223, 164-178, 2018.

[16] Mancini M., Buczynski R., Weber R., Fleck S., Stoesser P., Kolb T.: *Gasification of glycol: measurements and mathematical modelling*, 25. Deutscher Flammentag – Verbrennung und Feuerung: VDI Berichte 2119, 221-226, Karlsruhe, 2011.

[17] Mancini M., Weber R., Weigand P., Leuckel W., Kolb T.: *Design of the entrained flow reactor for gasification of biomass based slurry*, 26. Deutscher Flammentag – Verbrennung und Feuerung: VDI Berichte 2119, 625-634, Duisburg, 2013.

[18] Fleck, S., Hotz, C., Stoesser, P., Kolb, T.: *Gasification of biomass-based suspension fuels in an atmospheric entrained flow gasifier*, 27. Deutscher Flammentag – Verbrennung und Feuerung: VDI Berichte 2267, 207-217, Clausthal-Zerllerfeld, 2015.

[19] Dammann, M., Mancini M., Fleck, S., Weber R., Kolb, T.: *Entrained flow gasification: experiments and mathematical modelling based on RANS*, Joint Meeting of the German and the Italian Section of the Combustion Institute / 41st Annual Meeting of the Italian Section, Sorrent, 2018.